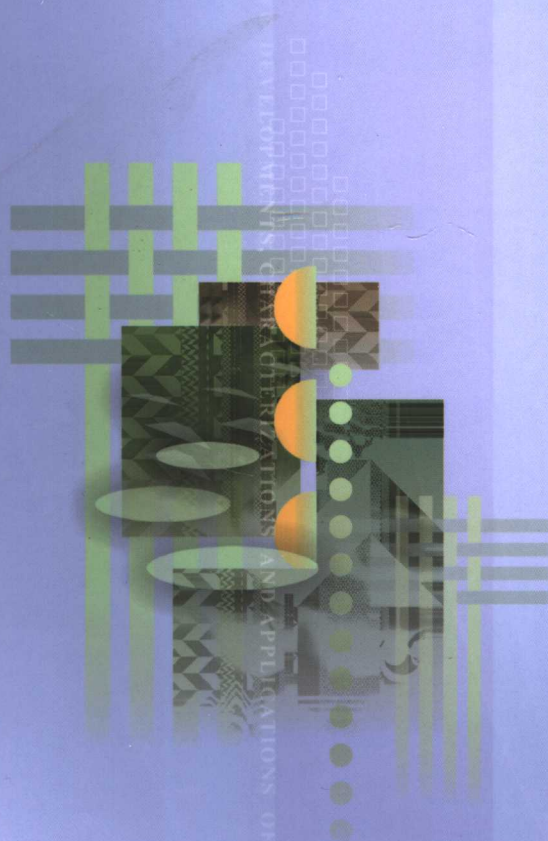


INNOVATIVE DEVELOPMENTS, CHARACTERIZATIONS AND APPLICATIONS OF COMPOSITES

Edited by Yao Zhang Qing-Qing Ni



CHINA AGRICULTURAL SCIENCE & TECHNOLOGY PRESS

INNOVATIVE DEVELOPMENTS, CHARACTERIZATIONS AND APPLICATIONS OF COMPOSITES

Edited by Yao Zhang Qing-Qing Ni



江苏工业学院图书馆
藏书章

CHINA AGRICULTURAL SCIENCE & TECHNOLOGY PRESS

图书在版编目(CIP)数据

复合材料表征与应用的新进展/张耀,倪庆清主编.
—北京:中国农业科学技术出版社,2006.7
ISBN 7-80167-999-7

I. 复… II. ①张…②倪… III. 复合材料—研究
IV. TB33

中国版本图书馆 CIP 数据核字(2006)第 078093 号

责任编辑: 刘 建

责任校对: 贾晓红

出 版 者: 中国农业科学技术出版社
北京市中关村南大街 12 号 邮编: 100081
电话: (010)62121118(编辑室)
(010)68919703(读者服务部)

传真: (010)68919709

社 网 址: <http://www.castp.cn>

经 销 者: 新华书店北京发行所

印 刷 者: 北京科信印刷厂

开 本: 787mm × 1092mm 1/16

印 张: 25.25

字 数: 600 千字

版 次: 2006 年 7 月第一版

印 次: 2006 年 7 月第一次印刷

印 数: 1 ~ 600 册

定 价: 150.00 元

INTERNATIONAL SCIENTIFIC COMMITTEE

Chairmen :

Yao ZHANG	Beihang University (China)
Goichi BEN	Nihon University (Japan)
Yan YING	Beihang University (China)
Qingqing NI	Shinshu University (Japan)

Steering Committee :

Farong HUANG	(China)	Yuxing DUAN	(China)
Kiyoshi KEMMOCHI	(Japan)	Hiroyuki KAWADA	(Japan)
Guangjie ZHAO	(China)	Guanfeng LIU	(China)
Tustao KATAYAMA	(Japan)	Ken KURASHIKI	(Japan)
Yiping QIU	(China)	Jialu LI	(China)
Jianhui QIU	(Japan)	Masaharu IWAMOTO	(Japan)
Xiaoquan CHEN	(China)	Wei SUN	(China)
Hideki SEKINE	(Japan)	Juhachi ODA	(Japan)
Yan ZHAO	(China)	Mikio MORITA	(Japan)
Tadashi SHIOYA	(Japan)	Takashi MATSUOKA	(Japan)
Lixia JIA	(China)	Takao TANAKA	(Japan)
Nobuo TAKEDA	(Japan)	Takayuki KUSAKA	(Japan)
Wenhua Lü	(China)	Yutaka ARIMITSU	(Japan)
Yoshihiro YAMASHITA	(Japan)	Akio SAKURAI	(Japan)
Zixing LU	(China)	Wen - Xue WANG	(Japan)
Satoshi SOMIYA	(Japan)	Hironori NAMIKI	(Japan)

TECHNICAL REVIEWERS

Zhao Yan	Beihang University
Cheng Xiaoquan	Beihang University
Cai Hong	Chinese Society of Composite Materials
Zhou Jun	Beihang University

SPONSORS

Chinese Society of Composite Materials (CSMS)
Japanese Society of Composite Materials (JSMS)

PREFACE

Since the Chinese Society for Composite Materials (CSCM) and the Japanese Society for Composite Materials (JSCM) sponsored the China-Japan Joint Conference on Composites (CJJCC) in 1997, six conferences (CJJCC 1 ~ 6) have been successfully launched in China or Japan, which provided an excellent base for scholars from both sides to present their achievements, exchange innovative ideas and share technical information. Following the steps of earlier joint conferences, the CJJCC - 7 will be held in Dunhuang, China from August 6th to 9th, 2006.

After critical reviews, over 50 high quality papers have been selected for presentation in the conference and for the publication in this book. The full papers selected in this book cover a wide range of topics, as Nanocomposites & Nanomechanics; Material & Processing; Properties & Characterization; Structure, Design & Analysis; Measuring & Computation, etc. It is believed that these current researches will offer us valuable information and will be beneficial to technique exchange among scientists and engineers.

The editorial committee would like to express their appreciation to many organizations and individuals who had contributed to the successful completion of the book. Among them are Chinese Society of Composite Materials (CSMS) and Japanese Society of Composite Materials (JSMS). In addition, we also would like to thank Prof. Hong CAI and the related members for their administrative and technical support.



Editor

Yao Zhang

Professor

Beihang University (China)

CONTENTS

Nanocomposites & Nanomechanics

- Preparation of Ferroelectrics/Polyethylene Nanocomposites by In-situ Polymerization
..... Tomoaki Karaki, Zhang Fan, Masatoshi Adachi, Li Sanxi (1)
- Preparation of Polyacrylonitrile/Montmorillonite Nanocomposite
..... Feng Huixia, Wang Yi, Fu Gongwei, Qiu Jianhui (10)
- Reinforcement Effect of Resin Material by a Small Amount of Carbon NANO Fiber
(VGCF) Additive Yoshihiro Yamashita, Toshimitsu Takahashi, Akira Tanaka (15)
- Preparation and Characterization of Water-Soluble PF/MMT Nanocomposites
..... Lü Wenhua, Zhao Guangjie (23)
- Physical and Mechanical Properties of Wood/MMT Intercalation Nanocomposites
..... Zhao Guangjie, Lü Wenhua (30)
- Mechanical and Electrical Properties of Carbon Nanotubes/UPR Nanocomposites
..... Ni Qingqing, Wu Shihong, Toshiaki Natsuki, Ken Kurashiki,
Guangze Dai, Masaharu Iwamoto (36)
- Microscopic Deformation Observation of Carbon Nanotubes-Poly(ether ether ketone)
Composites by In-situ SEM and TEM Deng Fei, Toshio Ogasawara, Nobuo Takeda (44)

Materials & Processing

- Recent Research Development of Polypropylene/Cellulose Composite Zhang Yingchen (51)
- Research Progress on Resin Precursor of Carbon-carbon Composites
..... Zhou Hongying, Zou Wu, Liu Jianjun, Cheng Wen, Wang Kai (59)
- Studies on the Compatibility of Polymer Composites with Liquid Oxygen
..... Wang Ge, Li Xiaodong, Guo Wei, Li Gongyi, Tang Yun (66)
- Preparation and Properties of a Novel Polytriazole Resin and Its Carbon Fiber Reinforced
Composite Wan Liqiang, Tian Jianjun, Xue Lian, Huang Jianzhi,
Hu Yanhong, Huang Farong, Du Lei (71)
- Study on Shelf Life of New Inorganic Ablative-Resistant Matrix
..... Tang Hongyan, Wang Jihui (77)
- Study on Process of GF/PP Warp-knitting Fabrics
..... Zhao Yan, Duan Yuexin, Zhang Yadong (82)
- Synthesis and Properties of PMR Polyimide Matrix Resins and Their Carbon Fiber-Reinforced
Composites Chen Jiansheng, Yang Shiyong, Hu Aijun, Fan Lin (89)

Development of Carbon Fiber Reinforced Aluminum Laminates

..... Wang Wenxue, Yoshihiro Takao, Terutake Matsubara (94)

Effects of Molecule Orientation on Mechanical Properties of PC/LCP Blends

..... Qiu Jianhui, Feng Huixia, Tetsuo Kumazawa,
Masayoshi Kitagawa, Makoto Kudo, Satoru Kamata, Mikio Morita (104)

Preparation and Mechanical Properties of Electrical Conductive Polyaniline Composites

..... Qiu Jianhui, Feng Huixia, Nie Furong, Huang Yudong, Pan Yubai (114)

Development of Life-Controllable Smart (LCS) Concrete Using Recycled PET Resin Blocks

..... Takayuki Kusaka, Hironori Namiki, Kei Urabe,
Hiromasa Takeno, Yukio Tada, Keiko Watanabe, Kensuke Okubo (123)

Development of Flexible Soundproof Material and Its Sound Characterization

..... Ni Qingqing, Lu Enjie, Naoya Kurahashi, Ken Kurashiki,
Kazunari Morimoto, Fu Yaqin, Masaharu Iwamoto (132)

Development and Damping Properties of Hybrid Laminates with Shape Memory Polymer

..... Zhang Chunsheng, Ni Qingqing, Wang Wenxue, Ken Kurashiki, Masaharu Iwamoto (141)

Study on Improving Drying Quality of Small-Diameter Lumbers with Intermittent-Heating

Method Guo Ming hui, Zhao Xiping, Yang Haili (150)

Properties & Characterization

The Study of Heat Resistant Properties of S₂/Ep Composite materials

..... Chen Hui, Yu Jinsheng, Jia Lixia, Jiao zhiwu (157)

Tensile and Dielectric Properties of Three-dimensional Orthogonal Woven Aramid-Glass

Fiber/Epoxy Composites L. Yao, W. B. Li, Y. P. Qiu (161)

Cure Dependent Stiffness of Plain Woven Fabric Composites

..... Yan Shilin Yang Mei (167)

Preparation and Properties of 3D Needled Carbon/Silicon Carbide Friction Materials

for Aircraft Application Fan Shangwu, Xu Yongdong, Zhang Litong,
Cheng Laifei, Lou Jianjun, Zhang Junzhan (174)

Study of High Flammable Resistant and Low Smoke Emission SMC

..... Sun Wei, Zheng Xusen, Zhai Guofang, Wang Jihui (182)

Influence of the Strain Rate on the Compression Behavior of 3D Kevlar/Epoxy

Woven Composites Xu Guo, Wang Li, Qiu Yiping (187)

Tension Properties of 3D Fabrics at Low Strain

..... Yang Caiyun, Li jialu (191)

Flame Retardancy of Paulownia Wood and its Mechanism

..... Li Peng, Juhachi Oda (197)

Friction Coefficient of Cluster Diamond-Dispersed Aluminum Composite

by Compression Shearing Method Noboru Nakayama, Hiroyuku Takeishi (206)

Fatigue Life Evaluation of GFRP by Infrared Thermography

..... Ken Kurashiki, Daisuke Tsuruga, Teruo Kimura, Masaharu Iwamoto (215)

High-cycle Fatigue Characteristics of CFRP Laminates Containing an Open Hole

..... Atsushi Hosoi, Keiichi Nagata, Yasuhiro Sakamoto and Hiroyuki Kawada (223)

Fracture Modes of C/C Composites at Elevated Temperature

..... Tadashi Shioya, Koji Fujimoto, Aya Kanai (231)

Bending Creep Behavior of Glass Fiber Reinforced Polyoxymethylene

..... Satoshi Somiya, Koichi Yamada, Takenobu Sakai (239)

Estimation of GRFP Residual Strength in Sulfuric Acid Environments Using X-ray

Analytical Microscope

..... Kazuto Tanaka, Yohei Kinoshita, Kohei Fukuchi, Tsutao Katayama (250)

Effect of Post-cure Time on Damage Progress of Plain Woven Glass Fabric Composites

..... Takao Ota, Takashi Matsuoka, Kazuhiko Sakaguchi (259)

Effects of YAG Laser Cutting and Post Heat Treatment on Stretch-flangeability of

0.1% ~0.4% C TRIP Steels

..... Akihiko Nagasaka, Koh-ichi Sugimoto, Yoichi Mukai, Yuichi Kubota (268)

A Comparative Study of Flake Alignment Distribution and Linear Expansion of Commercial

Oriented Strandboard Han Guangping, Cheng Wanli, Wu Qinglin (276)

Mechanical Properties of Straw/Polystyrene Composite Xu Min (282)

On the Cryogenic Tensile Strength of Polyimide Composite Film

..... Fu Shaoyun, Li Yan, Xu Guanshui (288)

The Effect of Moisture Absorption on Property of Epoxy/Cyanate Ester/Glass Cloth Composite

..... Huang Li, Wang Chen (295)

Structure, Design & Analysis

Studies on the Impact Performance of 3D Woven Composites

..... Tian Wei, Li Yanqing, Tan Dongyi, Chen Junjun, Zhu Chengyan (300)

Experimental Investigation of Stitched T-Section Composites Structures

..... Liu Bingshan, Yan Ying, Wang Lipeng (306)

Experimental Studies on Properties of Stitched Laminates Under Environment Conditions

..... Ali Al-Mansour, Cheng Xiaoquan, Chen Gang, Li Songnian (313)

Failure Load Predication for Load-Bearing joints of 3-Dimensional Braided Composites

..... Guo Yingnan, Zheng Xitao, Sun Qin, Chai Yanan, Li Xinxiang (320)

Experimental study on the warpage rule of unsymmetric composite Laminates

..... Li Min, Zhang Baoyan (325)

Study on the Post Buckling and Durability/Damage Tolerance of Composite Stiffened Panels

with Different Thickness Li Gelan, Wu Bin (331)

Trial Manufacture of FRP Craft by Resin Infusion Processing Akio Sakurai, Masao Ono (337)

Optimization of Material Distributions for Minimizing the Stress Intensity Factor in Multi-Phase

FGM Circular Pipes under Thermomechanical Loading Kimiaki Yoshida, Hideki Sekine (344)

Computer Aided Filament-wound for Non-geodesic Winding Toroidal Pressure Vessels

..... Zu Lei, He Qinxiang, Li Fuan (352)

Strain Rate and Temperature Effects on the Nonlinear Behavior of Woven Composites

..... Liqun Xing, Ken Reifsnider, X. Huang (363)

Measuring & Computation

Study on Real-time Monitoring Technique of LCM Process

..... Duan Yuexin, Zhao Yan, Zuo Lu, Zhang Zuoguang (371)

The Fast Determination of Moisture Content, Combustible Matter Content, Mass Per Unit Area

and Linear Density for Reinforcement of Fiber Glass, Fabric and Mat Wang Xiumei (377)

Finite Element Method for Microstretch Elastic Solids

..... Yutaka Arimitsu, Shigeyuki Nakano, Hiroto Kawano, Yuji Sogabe, Wu Zhiqian (383)

PREPARATION OF FERROELECTRICS/POLYETHYLENE NANOCOMPOSITES BY IN-SITU POLYMERIZATION

Tomoaki Karaki¹, Fan Zhang^{1,2}, Masatoshi Adachi¹, Sanxi Li³

¹*Faculty of Engineering, Toyama Prefectural University, Toyama 939-0398, Japan*

²*School of Materials Science and Engineering,*

Shenyang Institute of Chemical Technology, Shenyang 110142, China

³*Shenyang University of Technology, Shenyang 110023, China*

Abstract Nanosized perovskite ferroelectric lead strontium titanate ($\text{Pb}_x\text{Sr}_{1-x}\text{TiO}_3$ (PST)) powders were successfully prepared by a simple coprecipitation method. Lead-strontium titanyl oxalate (PSTO) precursor was first synthesized at room temperature, and the precursor was then calcined at a temperature higher than 600°C for 1 h to produce the single-phase perovskite PST powders. The average diameter was ranging from 10 to 200 nm. PST powders with desired composition could be synthesized by adding 25 mol% excess Sr. Then, Ziegler-Natta catalysts were supported on the PST powders and PST/polyethylene (PST/PE) nanocomposites were prepared by in-situ polymerization. PST/PE nanocomposites with different volume fractions of PST were obtained by changing the polymerization time. The dispersion and element distribution of the PST powder in the PST/PE nanocomposite were investigated by analyses and observations of energy dispersion X-ray (EDX) and transmission electron microscopy (TEM). The results indicated that the PST powder homogeneously dispersed in the PE matrix. The dielectric properties and Curie temperatures of the PST powders and PST/PE nanocomposites were also evaluated.

Key words Ferroelectrics; Coprecipitation; In-situ polymerization; Nanocomposite

INTRODUCTION

($\text{Pb}_x\text{Sr}_{1-x}\text{TiO}_3$ (PST)) is a complete solid solution of PbTiO_3 (PT) and SrTiO_3 (ST), and has a perovskite structure just like ($\text{Ba}_x\text{Sr}_{1-x}\text{TiO}_3$ (BST)). The Curie temperature of PST could be adjusted by the ratio of PT and ST from -220 to 490°C, so is called composition-dependent Curie temperature. Due to its large electric field-dependent dielectric constant at a temperature near the Curie temperature, the PST is highly suitable for electronic and microelectronic applications, such as microwave devices, frequency tuning devices, capacitors, sensors, etc^[1,2]. For ferroelectrics, the important electromechanical properties are the result of structural and micro structural changes that are incurred at Curie temperature. Size-effect phenomena issues in ferroelectrics have been of interest for many years. However, despite a large number of recent investigations regarding the effect of size on the ferroelectric

transition^[3,4], few studies that focused on the nanosized PST powders with various stoichiometric compositions and particle sizes have been reported. Curie temperature of most ferroelectric materials drops remarkably when the particle size decreases to less than 100 nm, so is called the size effect^[5,6]. Obviously, the PST is one of the most suitable candidates for nano-ferroelectrics applications in nano-electromechanical-system (NEMS), since its Curie temperature could be compensated by the composition. Therefore, preparation and evaluation of nanosized PST powders have been getting an increasing interest because of their novel physicochemical properties, which might be quite different from those of the bulk materials.

The ferroelectric materials have spontaneous polarization that causes particle agglomeration particularly in these nanosized powders. Dispersing the PST powders in a select polymer is an advantageous way for the solution as well as its applications. Polyethylene (PE) belongs to polyolefin that is one of the fastest growing classes of thermoplastics. Polyethylene/montmorillonite (PE/MMT) nanocomposites had been prepared via in-situ intercalative polymerization of ethylene after supporting Ziegler-Natta catalysts on the silicate MMT^[7]. It indicated that ethylene could be polymerized on the surface of oxides to form PE/oxide composites. Therefore, it is possible to prepare (Pb, Sr) TiO₃/polyethylene (PST/PE) nanocomposites by the in-situ polymerization method.

In this paper, the nano-powders of ferroelectric PST were synthesized by coprecipitation processing, and then the PST/PE nanocomposites were prepared via in-situ polymerization. The process, structure and properties of PST powders and PE/PST nanocomposites were examined by various methods.

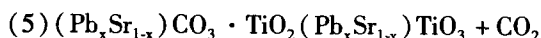
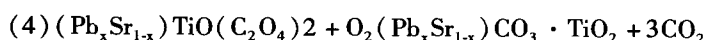
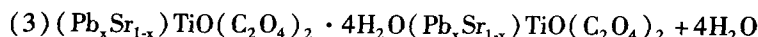
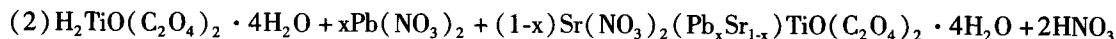
PREPARATION AND PROPERTIES OF NANOSIZED PST POWDERS

The starting materials were oxalic acid, ethanol, titanium tetrabutoxide, lead nitrate and strontium nitrate. Initially, H₂C₂O₄ · 2H₂O and Ti(OC₄H₉)₄ were dissolved in ethanol, respectively. The Ti(OC₄H₉)₄ solution was then added into oxalic acid solution at room temperature, resulting in a clear oxalatitanic acid solution, H₂TiO(C₂O₄)₂ · 4H₂O (HTO). Mixed aqueous solution of Pb(NO₃)₂ and Sr(NO₃)₂ was dripped slowly into the HTO with a constant stirring. The pH value of the solution was adjusted by adding aqueous ammonia and/or nitric acid. The resulting micro emulsion-derived precursor was kept overnight for the reaction to go to its completion. The precipitate, (Pb, Sr) TiO(C₂O₄)₂ · 4H₂O (PSTO) obtained was filtered, washed, dried and calcined. Finally, PST crystalline powders were obtained^[8].

Due to the different solubility of constituent components in the coprecipitation system, the final composition in the product is not always consistent with that of the starting materials introduced in the beginning. The pH value has obvious effect on the chemical composition. In this work, the products with starting compositions of PT, ST and (Pb_{0.5}Sr_{0.5})TiO₃ (PST5/5) were analyzed by Energy Dispersion X-ray (EDX) and Inductively Coupled Plasma (ICP). The results showed that stoichiometric PT powder could be obtained by this method with pH = 1, but the Sr/Ti ratio of ST powder changed from

0.80 at pH = 1 to 0.95 at pH = 4. Considering all the results from the analyses, it was found that an excess amount of 25 mol% Sr was required to obtain PST powders with desired composition at pH = 1. Hence, an excess of 25 mol% $\text{Sr}(\text{NO}_3)_2$ was added to starting materials in order to synthesize PST powders with desired composition at pH = 1 for all the further investigation in our work.

The complete reaction process could be expressed as below:



From the above formulas, thermal decomposition of PSTO precursor was the main process by heating it in air/oxygen atmosphere, as represented in reactions(3)-(5). To study this process, thermogravimetric and differential thermal analyses (DTA/TGA), Fourier transform infrared spectrometer (FTIR)

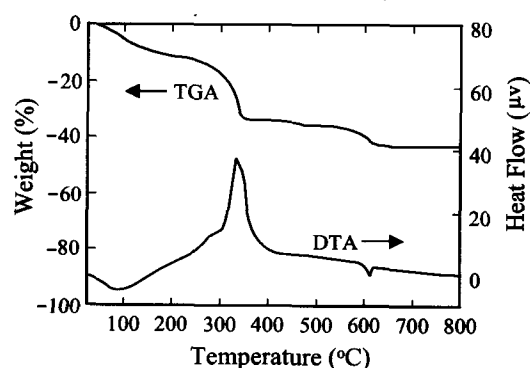


Fig. 1. DTA/TGA curves of PSTO.

(b), it was clear that the absorption bands of oxalate group around $1725 \sim 1633$, 1420 and 1280 cm^{-1} in PSTO were absent in $(\text{Pb}, \text{Sr})\text{CO}_3 \cdot \text{TiO}_2$ ^[9,10]. In curve(b), there were a band at 2340 cm^{-1} related to CO_2 adsorbed on a metal cation, and a sharp band at 1480 cm^{-1} assigned to unidentified carbonate^[11]. The FTIR spectrum curve(c) did not show any band between 4000 and 1000 cm^{-1} . The room-temperature XRD patterns of PST5/5 calcined in air for 1 h at various temperatures indicated its phase development, as shown in Fig. 3. It also can be seen that PST5/5 powders calcined below 900°C have a cubic structure while those samples cal-

and X-ray diffractometer (XRD) were carried out. According to TGA and DTA curves in Fig. 1, there are three stages of weight loss, which appear in the temperature range from room temperature to 250°C , from 250°C to 400°C , and around 600°C . The experimentally observed weight losses were in good agreement with the theoretically calculated values based on the thermal reactions. Figure 2 shows curves of FTIR for PSTO, $(\text{Pb}, \text{Sr})\text{CO}_3 \cdot \text{TiO}_2$ calcined at 400°C for 1h and the final PST calcined at 600°C for 1h. In comparison of the curves (a) and

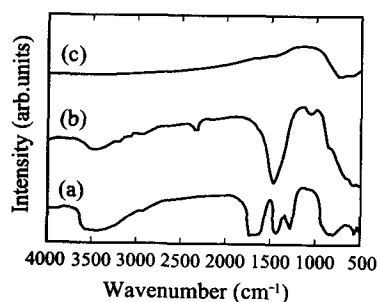


Fig. 2 FTIR spectra of (a) PSTO, (b) $(\text{Pb}, \text{Sr})\text{CO}_3 \cdot \text{TiO}_2$ and (c) PST.

cined at 1 000°C have a tetragonal one at room temperature.

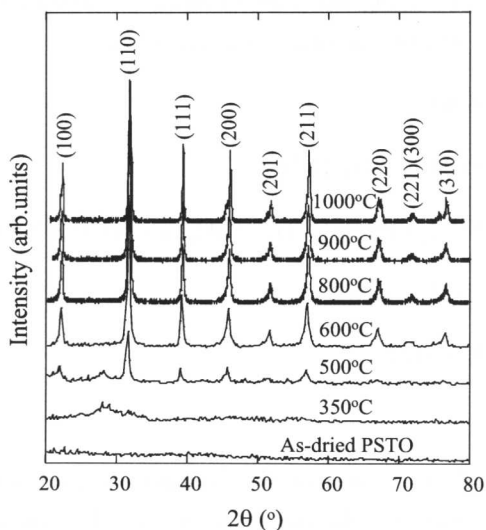


Fig. 3 Room – temperature XRD patterns of PST5/5 powders calcined at various temperatures.

A transmission electron microscopy (TEM) was used to analyze the particle size and morphology of the PST powders. The PST powders were treated with ball milling in ethanol for dispersion before TEM observation. Figure 4 shows the TEM photographs of PST5/5 powders calcined at 600 (a) and 1 000°C (b) for 1 h, respectively. From the pictures, PST5/5 powders were of spherical in nature with average sizes of 10 and 200 nm. In this way, the average particle sizes of PST5/5 as well as $(\text{Pb}_{0.6}\text{Sr}_{0.4})\text{TiO}_3$ (PST6/4) and $(\text{Pb}_{0.7}\text{Sr}_{0.3})\text{TiO}_3$ (PST7/3) powders were estimated, as shown in Fig. 5. Therefore, the particle size could be controlled in range of 10 ~ 200 nm by varying the calcination temperature from 600°C to 1 000°C.

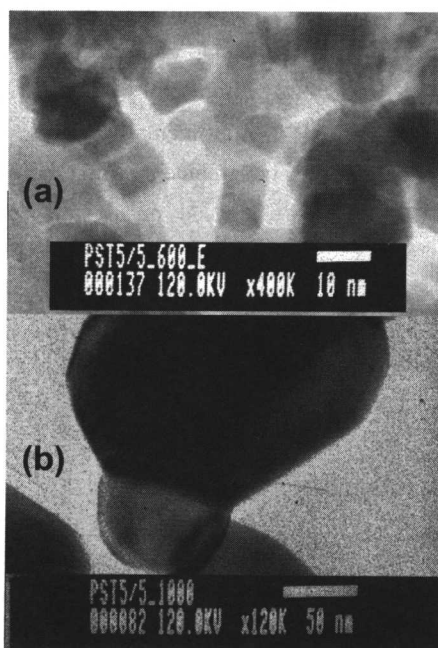


Fig. 4 TEM photographs of PST.

Using high-temperature XRD, the Curie temperatures of PST powders were estimated. The temperature at which the splitting of (002) and (200) refraction peaks around $2\theta = 45^\circ$ disappeared was taken

as the Curie temperature. Figure 6 shows the dependence of Curie temperature on the particle size for PST6/4. The Curie temperature of a sample below 200 nm in size decreased sharply as the particle size decreased. These Curie temperatures are much lower than that of the bulk PST6/4, 230°C^[1]. For nanosized powders, the crystalline size is so small that thermal vibrations at a lower temperature may destroy the ordered anisotropic crystalline structure. This results in the disappearance of ferroelectricity and a decrease of the Curie temperature. The surface tension effect has been also used to explain the observations. The large internal pressure caused by the particle size would qualitatively shift the Curie temperature to a lower temperature for ferroelectric materials.

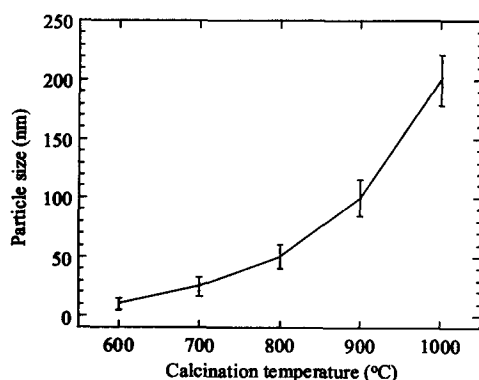


Fig. 5 Size dependence on calcination temperature.

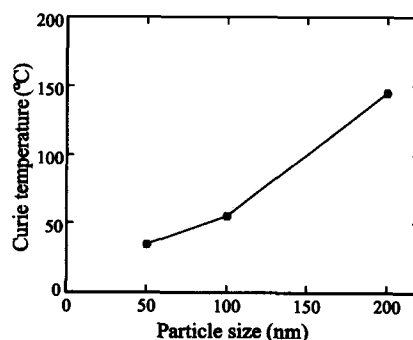


Fig. 6 Curie temperature of PST6/4 dependence on particle size.

PREPARATION AND PROPERTIES OF PST/PE NANOCOM-POSITS

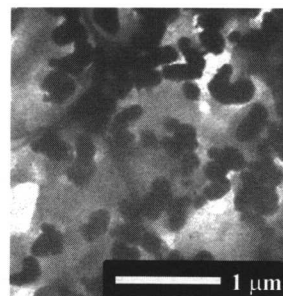
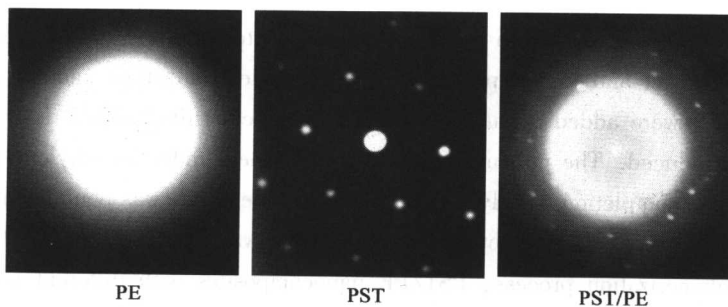
In an N₂-purged 250 ml four-neck glass reactor fitted with a stirrer, the prepared PST6/4 powder 100 nm in size and anhydrous heptane were introduced and the mixture was then stirred to a homogeneous suspension. TiCl₄ was added dropwise to the suspension over 1 h at room temperature and the reaction was allowed to continue for another 2 h. The obtained slurry was then separated by filtration, and the residual was washed several times with heptane. The PST-supported catalyst was then stored in ampoules as slurry in heptane.

Slurry polymerization was carried out in a 5 L autoclave reactor equipped with a mechanical stirrer. Alkyl aluminum cocatalyst and the prepared slurry with Ziegler-Natta-type catalyst supported on the nanosized PST powder were added in succession into the reactor filled with 2 L of hexane and then ethylene gas was introduced. The polymerization was performed under an ethylene gas pressure of 1 bar at 60°C. After the completion of polymerization, the whole slurry was poured into a large container and the solvent was decanted. The obtained solid polymer was collected and dried in vacuum. During the ethylene polymerization process, PST/PE nanocomposites with different volume fractions of PST were obtained by changing the polymerization time, as listed in Table 1.

Table 1 Ethylene polymerization results

	Polymerization time(min)	PST content(wt%)	Volume fraction of PST(%)
PST/PE-1	20	24.3	4.1
PST/PE-2	10	36.6	7.2
PST/PE-3	5	55.8	14.5
PST/PE-4	3	84.2	41.9

The TEM photograph in Fig. 7 shows the PST/PE nanocomposite. The black particles are the PST powders and the lighter areas belong to the PE matrix. It could be seen that the PST particles in the nanocomposites are dispersed separately. Figure 8 shows the electron diffraction patterns of the PE, PST and PST/PE. PE is a partial crystalline polymer with a spherulite structure, which consists of aggregates of lamellar crystals formed by folding molecular chains. From the figure, the electron diffraction pattern of PE consists of dispersed concentric rings. PST is monocrystalline and its electron diffraction pattern is made up of regularly lined lattices. In the diffraction pattern of PST/PE, dispersed concentric rings and regularly lined lattices are superimposed. The elemental distribution of the PST/PE nano-composite was examined by a scanning electron microscopy (SEM). In Figure 9, the white particles of PST6/4 powders 100 nm in size are dispersed in the black PE matrix. The distributions of elements such as Pb, Sr, Ti and O in PST are clearly observed. All of the above results indicate that PST powders homogeneously dispersed in the PE matrix during ethylene polymerization and that a uniform PST/PE nanocomposite was formed. The phase of PST/PE nanocomposite with various volume fractions was evaluated by XRD, as shown in Fig. 10. Pure PE shows strong X-ray diffraction peaks in the 2θ angle range of $20^\circ \sim 25^\circ$. The PST perovskite structure is visible as soon as PST powders exist in the PE matrix. With increasing volume fraction of the PST powders, the characteristic diffraction peaks of PST6/4 become stronger and those of PE gradually fade out. This corroborated the formation of PST/PE nanocomposites.

**Fig. 7** TEM photograph of PST/PE nano-composite.**Fig. 8** Electron diffraction patterns of PE, PST6/4 and PST/PE.

In this study, the dielectric constant of PST6/4 powders 100 nm in size was estimated to be 849 at 20°C by the powder dielectric measurement method^[12]. The dielectric constant of PE is known to be 2.3. The dielectric constants of PST/PE nanocomposites with different volume fractions of PST60/40 powders were evaluated at 20°C and 100 kHz. Figure 11 shows the dependence of the dielectric constant of PST/PE nanocomposites on the volume fraction of PST6/4. From the TEM photograph in Fig. 7, it can be seen that the PST particles are almost separated and surrounded by the PE matrix in the nanocomposite. The 0-3-type composite model is most applicable to the nanocomposites. Yamada et al. proposed a theoretical model to explain the behavior of the dielectric properties for 0 ~ 3 composites^[13]. The dielectric constant of

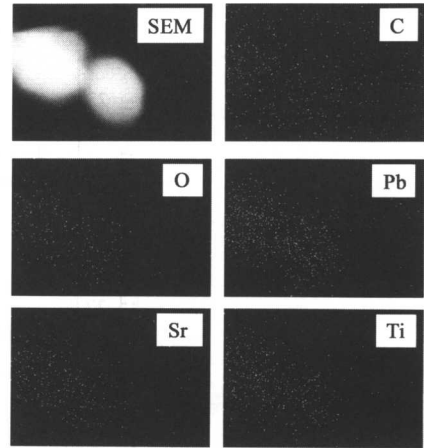


Fig. 9 SEM image and elemental distribution for PST/PE.

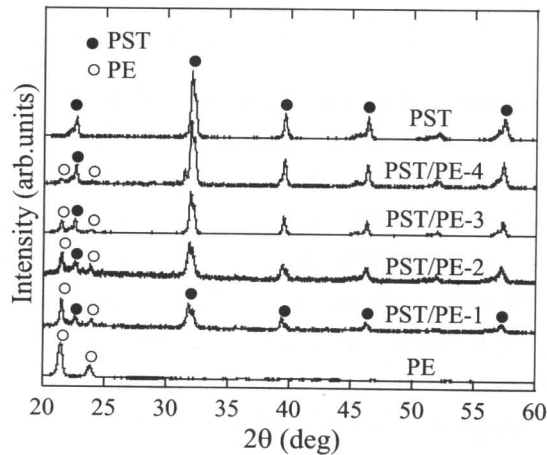


Fig. 10 XRD patterns of PST/PE with various volume fractions of PST6/4.

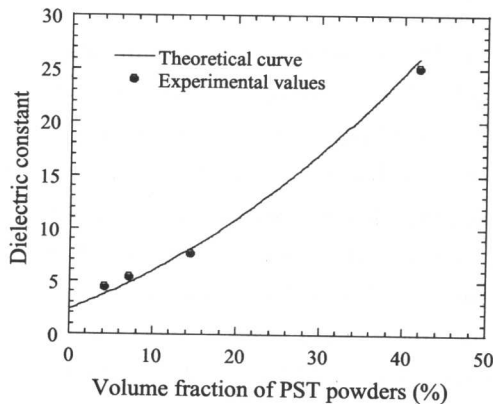


Fig. 11 Dependence of dielectric constant of PST/PE on volume fraction of PST6/4.

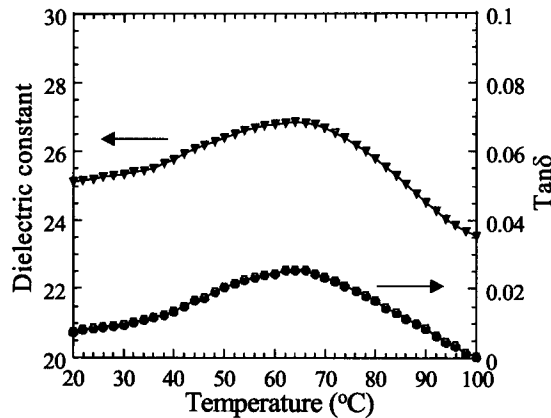


Fig. 12 Dependence of dielectric constant of PST/PE -4 on temperature.

the composite is given by

$$\varepsilon = \varepsilon^p \left\{ 1 + \frac{\eta \phi (\varepsilon^c - \varepsilon^p)}{\eta \varepsilon^p + (\varepsilon^c - \varepsilon^p) (1 - \phi)} \right\}$$

where η is a parameter depending on the shape of particles and ϕ is the volume fraction of the ceramic. The other symbols ε , ε^c and ε^p refer to the magnitudes of the dielectric constants of the composite, ceramic and polymer, respectively. In this study, a shape parameter equal to 15.5 was found to fit to our experimental values obtained in PST/PE composites with various ceramic volume fractions. Figure 11 reveals that the dielectric constants of PST/PE appear to have strong concentration dependence and are in good agreement with theoretical values. Figure 12 shows the dielectric constant of PST/PE-4 in the temperature range from 20 to 100°C and measured at 100 kHz. There is a maximum at 64°C, which implies the Curie temperature of PST6/4 powders was about 64°C. This value corresponded with that estimated by high-temperature XRD (Fig. 6).

CONCLUSION

Nanosized perovskite ferroelectric PST powders were successfully prepared the coprecipitation method. The completed reaction process for the preparation was characterized. The PST powders with desired composition could be synthesized by adding 25 mol% excess Sr. The average diameter was ranging from 10 to 200 nm by means of controlling the calcination temperature. The size effect on Curie temperature showed a sharply decreasing when the particle size decreased below 200 nm. Then, Ziegler-Natta catalysts were supported on the PST6/4 powders and PST/PE nanocomposites were prepared by in-situ polymerization. The volume fractions of PST powder in the nanocomposite could be adjusted by changing the polymerization time. By the SEM analyses and TEM observations, it was known that the PST powders homogeneously dispersed in the PE matrix during ethylene polymerization. The dielectric constant of PST/PE appeared to have strong concentration dependence. By the dependence of dielectric constant of PST/PE on temperature, the Curie temperature of PST6/4 powders was observed at